

Proceeding Paper

Absorption and dispersion properties of a coupled asymmetric double quantum dot molecule – metal nanoparticle structure [†]

Spyridon G. Kosionis* and Emmanuel Paspalakis

Materials Science Department, School of Natural Sciences, University of Patras, 265 04 Patras, Greece; paspalak@upatras.gr (E.P.)

* Correspondence: kosionis@upatras.gr; Tel.: +30-2610-996315.

[†] Presented at the 4th International Electronic Conference on Applied Sciences, 27 October–10 November 2023; Available online: <https://sciforum.net/event/ASEC2023>.

Abstract: The interaction of excitons with localized surface plasmons in hybrid nanostructures containing semiconductor quantum dots and metal nanoparticles, under specific conditions, might generate collective optical properties with an abundance of potential applications in the area of nanotechnology. In the present study, we explore the behavior of the linear absorption and dispersion properties of the double semiconductor quantum dot molecule in the presence of a spherical metal nanoparticle. We find that a transparency window arises on the absorption spectrum the width of which decreases with the decrease of the electron tunnelling rate. In the low electron tunnelling regime, slow light is generated, an effect closely associated with tunneling induced transparency. The enhancement of the tunneling rate induces a broadening in the transparency window, due to the Autler-Townes splitting. The investigation of impact of the distance between the quantum dot and the metal nanoparticle on the slow down factor and the width of the transparency window shows that by transposing the metal nanoparticle closer to the double semiconductor quantum dot molecule the transparency window widens.

Citation: To be added by editorial staff during production.

Academic Editor: Firstname Last-name

Published: date



Copyright: © 2023 by the authors. Submitted for possible open access publication under the terms and conditions of the Creative Commons Attribution (CC BY) license (<https://creativecommons.org/licenses/by/4.0/>).

Keywords: Absorption; Autler-Townes splitting; dispersion; hybrid nanostructure; metal nanoparticle; semiconductor quantum dot molecule; tunneling-induced transparency

1. Introduction

The potential properties arising from the interaction of semiconductor quantum dots (SQDs) with electromagnetic fields have been studied intensely in recent years for their applications in nanophotonics and quantum technologies. The asymmetric double semiconductor quantum dot molecule is a semiconductor quantum dot nanostructure that exhibits unique optical properties [1–6], leading, for example, to important quantum optical phenomena like tunneling induced transparency, Autler-Townes splitting and slow light generation without the need of an external electromagnetic field. When semiconductor quantum dots and metal nanoparticles (MNPs) are placed close to each other, with distances in a few nanometers range, coupled nanostructures are created that have, in many cases, enhanced optical properties in comparison to the individual components. Recently, attention has been given to the optical properties of a coupled nanostructure fabricated by coupling a metal nanoparticle to a double semiconductor quantum dot molecule [7–10].

In the present work, the behavior of the absorption and dispersion properties of the double semiconductor quantum dot molecule in the presence of a spherical metal nanoparticle is explored, by applying a theoretical approach. Specifically, tunneling induced transparency, Autler-Townes splitting, and slow light generation are obtained in the

double SQD structure under the presence of the metal nanoparticle and their properties on the interparticle distance between the semiconductor quantum dot structure and the metal nanoparticle is studied.

2. Methods

The hybrid nanostructure under study consists of a spherical MNP and an asymmetric double SQD molecule. The electric permittivities of the SDQs and the environment are denoted by ϵ_S and ϵ_{env} , respectively, while the electric permittivity of the MNP is described by the frequency-dependent function $\epsilon_m(\omega)$. We symbolize the center-to-center distance between the components of the hybrid with R and the radius of the MNP with a . The SQDs are assumed to have different band structures, while their coupling is achieved due to the coherent tunneling effect.

The hybrid nanostructure is subjected to a classical electromagnetic field with amplitude E and angular frequency ω , that excites the interband transition $|0\rangle \rightarrow |1\rangle$, as shown in Fig. 1. A continuum of states is used to model the surface plasmons induced on the MNP and the exciton states of the asymmetric double SQD molecule can be depicted as a characteristic Λ -type energy-level pattern: $|0\rangle$ is the ground state, $|1\rangle$ is the direct exciton state (the excited electron and the hole are both located in the same SQD) and $|2\rangle$ is the indirect exciton state (the excited electron is transferred to the second SQD, due to coherent electron tunneling, while the hole remains in the first SQD). The tunneling rate T_e is adjusted by modifying the value of a gate voltage applied to the SQDs. Long-range electrostatic interaction couples the SQDs to the MNP.

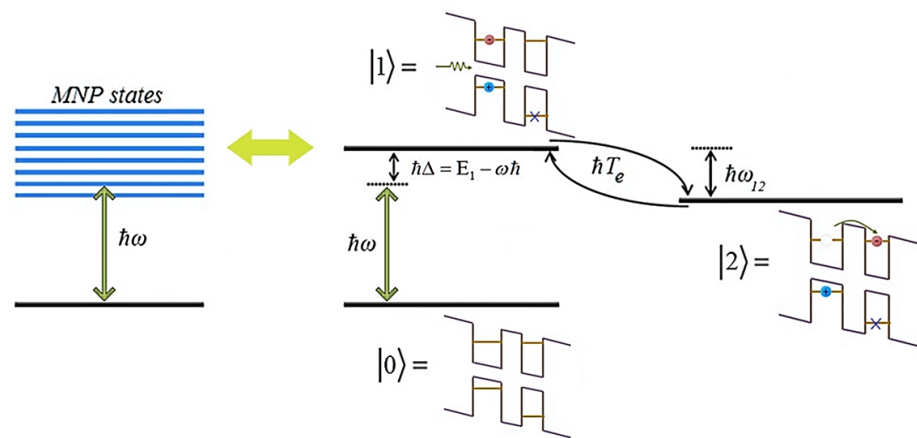


Figure 1. Schematic energy-level configuration of the double SQD molecule (right) and the MNP (left) coupled together via Coulomb interaction. The surface plasmons induced on the MNP are modeled as a continuum of energy states and the exciton states of the asymmetric double SQD molecule correspond to a typical Λ -type energy-level configuration.

The Hamiltonian of the system, in the dipole approximation, is written as a summation of the terms H_i , with $i = 1, 2, 3$. In this case, $H_1 = \sum_{n=1,2} E_n |n\rangle \langle n|$ describes the unperturbed Λ -type system, with E_n denoting the energy of state $|n\rangle$, while $H_2 = -\hbar \{ [G\rho_{10}(t) + \Omega] e^{-i\omega t} + c.c. \} (|0\rangle \langle 1| + |1\rangle \langle 0|)$ owes its presence to the coupling of the asymmetric SQD molecule with the incident field, where $G = \sum_{n=1}^N (s_n \gamma_n a^{2n+1} \mu^2) / (4\pi \hbar \epsilon_{env} \epsilon_{effS}^2 R^{2n+4})$ is related to the self-interaction of the SQD

molecule and $\Omega = \left[E\mu / (2\hbar\epsilon_{effS}) \right] \left(1 + s_a\gamma_1 a^3 / R^3 \right)$ is the Rabi frequency, with μ symbolizing the electric dipole moment of the $|0\rangle \leftrightarrow |1\rangle$ transition, $\epsilon_{effS} = (\epsilon_S + 2\epsilon_{env}) / (3\epsilon_{env})$ and $\gamma_n = \left[\epsilon_m(\omega) - \epsilon_{env} \right] / \left[\epsilon_{env}(n+1) / n + \epsilon_m(\omega) \right]$. Finally, $H_3 = \hbar T_e |1\rangle\langle 2| + c.c.$ counts for electron tunneling between the SQDs, where T_e is the tunneling rate coefficient.

Next, we derive the density matrix equations, under the rotating wave approximation, and apply a first-order expansion approximation to the density matrix elements, with respect to the amplitude of the probe field, $\rho_{nm} = \rho_{nm}^{(1)} + \Omega^* e^{i\omega t} \rho_{nm}^{(2)} + \Omega e^{-i\omega t} \rho_{nm}^{(3)}$, where $|\rho_{nm}^{(2)}|, |\rho_{nm}^{(3)}| \ll |\rho_{nm}^{(1)}|$, and obtain a set of differential equations, which are solved, in the steady state. In order to explore the linear optical response (dispersion and absorption) of the asymmetric SQD molecule to the probe field, we should calculate the real and the imaginary parts of the optical susceptibility

$$\chi_{SQD}^{(1)}(\omega) = \left[2(\Gamma/V)\mu / (\epsilon_0 E) \right] \rho_{01}^{(2)*}(\omega), \quad (1)$$

where (Γ/V) denotes the ratio of the squared electric field restricted in the active region of an SQD over the volume of an SQD.

The slow-down factor for the light propagating through the asymmetric SQD is

$$S(\omega) = n(\omega) + \omega \left[\partial n(\omega) / \partial \omega \right], \quad (2)$$

where $n(\omega) = \sqrt{\text{Re}[1 + \chi_{SQD}^{(1)}(\omega)]}$ is the index of refraction.

3. Results and Discussion

In Figs. 2 and 3, we investigate the profile of the linear dispersion, caption (a), and absorption spectra, caption (b), for the SQD, as a function of the field detuning $\hbar(\omega - \omega_{01})$ of the incident field with regard to the $|0\rangle \leftrightarrow |1\rangle$ transition, in two distinct electron tunnelling regimes ($\hbar T_e = 0.5 \text{ meV}$, in Fig. 2 and 0.15 meV , in Fig. 3). In Fig. 4, we present the slow down factor for the light propagating through the double SQD molecule, as a function of the detuning $\hbar(\omega - \omega_{01})$, for a high, caption (a), and a low, caption (b), electron tunneling rate. Discrete line-styles are used to indicate different values of the interparticle distance ($R = 11.5 \text{ nm}$: turquoise solid curve, 13 nm : magenta dashed curve and 80 nm : blue dotted curve). We use the values of the decay rates $\hbar\Gamma_{10} = 0.022 \text{ meV}$, $\hbar\Gamma_{12} = 0$, $\hbar\Gamma_{20} = 0.0001 \text{ meV}$ and the dephasing rates $\hbar\gamma_{01} = 0.22 \text{ meV}$, $\hbar\gamma_{12} = 0.1 \text{ meV}$, $\hbar\gamma_{02} = 0.001 \text{ meV}$, which are typical for InAs/GaAs SQDs. The nanostructure is surrounded by vacuum and the hybrid structure is placed in vacuum ($\epsilon_{env} = \epsilon_0$), and the electric permittivity of the SQDs is six times the one corresponding to vacuum ($\epsilon_S = 6\epsilon_0$), as in Ref. [8]. The dipole moment for the interband optical transition is $\mu = 0.65 \cdot e \text{ nm}$ and the energy difference between levels $|0\rangle$ and $|1\rangle$ is $\hbar\omega_{01} = 1.4 \text{ eV}$. In the strong confinement regime, we assume that $\Gamma/V = 5 \times 10^{23} \text{ m}^{-3}$ [8]. The polarization of the probe field is assumed to be in parallel with the interparticle axis and, hence, $s_a = 2$ and $s_n = (n+1)^2$. The MNP has a fixed size, with radius $a = 7.5 \text{ nm}$, while, for its electric permittivity function $\epsilon_m(\omega)$, we use the experimental data that correspond to gold, Ref. [10]. We found that it is sufficient to keep $N = 10$ terms, while applying the multipole polarization regime, in order to calculate the self-interaction coefficient G , since the results reach convergence.

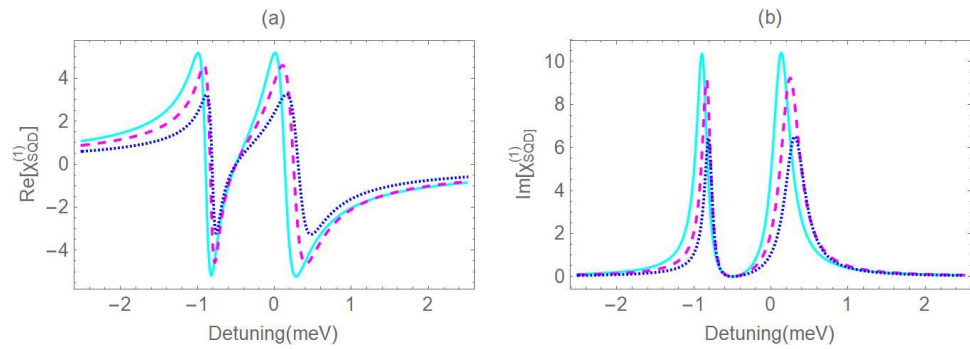


Figure 2. The spectra of the real and the imaginary part of $\chi_{SQD}^{(1)}$, captions (a) and (b), respectively, for various interparticle distances ($R = 11.5 \text{ nm}$: turquoise solid curve, 13 nm : magenta dashed curve and 80 nm : blue dotted curve), for a tunneling rate coefficient $T_e = 0.5 \text{ meV}$. The values of the rest physical parameters are provided in the section ‘Parameters and Results’.

In Figs. 2(a) and (b), we present the linear dispersion spectrum and absorption spectrum, for the SQD, respectively, for different values of the parameter R , in the strong tunneling regime, with $\hbar T_e = 0.5 \text{ meV}$. Considering an infinitesimal interaction between the components of the nanostructure, a condition practically accomplished at the distance of 80 nm , we observe that the spectral profile of $\text{Re}[\chi_{SQD}^{(1)}]$ ($/\text{Im}[\chi_{SQD}^{(1)}]$) is composed of two dispersion-like (Lorentzian-type) resonances centered at $\omega - \omega_{01} \approx -\omega_{12} / 2 - G_R / 2 \pm \sqrt{(\omega_{12} - G_R)^2 + 4T_e^2} / 2$, where $G_R = \text{Re}(G)$. The full width at half maximum (FWHM) of the resonances that arise on the spectrum of $\text{Im}[\chi_{SQD}^{(1)}]$ are given by the formulae $\left[1 \pm (\omega_{12} - G_R) / \sqrt{(\omega_{12} - G_R)^2 + T_e^2} \right] \gamma_{01}$. We also found that, in the limiting case where the upper states are degenerate ($\omega_{12} = 0$), the profiles of these spectra become antisymmetric and symmetric, respectively. In the general case, the value of $\text{Im}[\chi_{SQD}^{(1)}]$, at the position of its local minimum ($\omega - \omega_{01} \approx -\omega_{12}$) is

$$\text{Im}[\chi_{SQD}^{(1)}]_{\min} = 2 \left(\frac{\Gamma}{V} \right) \frac{\mu \Omega_R}{\epsilon_0 E} \frac{\gamma_{02}}{\gamma_{01} \gamma_{02} + T_e^2}, \tag{4}$$

which exhibits dependence on the interparticle distance, as the second term of the Rabi frequency is proportional to R^{-3} . The minimum absorption, which is found and leads to the phenomenon of tunneling induced transparency, cannot be equal to zero for a non-zero tunneling rate coefficient, since the first term of the Rabi frequency cannot be eliminated for any value of the interparticle distance, as it is R -independent. When the asymmetric SQD molecule is brought closer to the MNP, due to the increase of the G_R parameter, the distance between the resonances along the horizontal axis, and the difference of the FWHM that correspond to the resonances of the absorption spectrum should both increase, based on the analytical formulae given above.

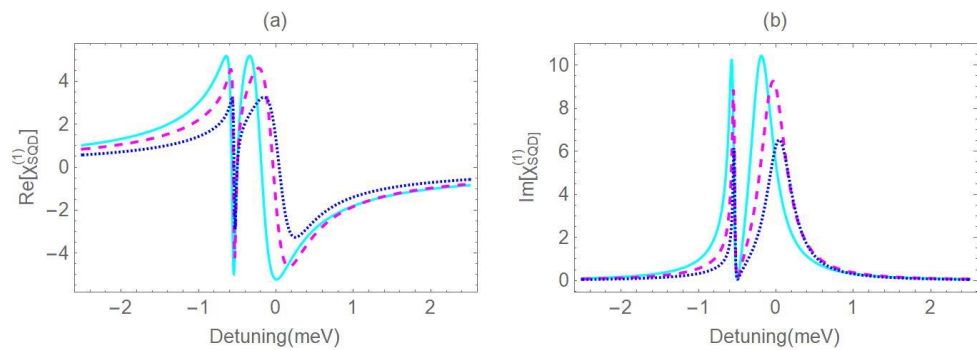


Figure 3. Same spectra as in Fig. 2, with $T_e = 0.15 \text{ meV}$.

In Fig. 3, we investigate the linear optical response of the SQD, for a lower electron tunneling rate ($\hbar T_e = 0.15 \text{ meV}$). We can show that the amplitude of maximal absorption is independent of the tunneling rate, which explains why the magnitude of the absorption resonances remains the same, for a given value of the parameter R , as the one detected in Fig. 2(b), with $\hbar T_e = 0.5 \text{ meV}$. Furthermore, the distance between the positions of the resonances and the discrepancy of the FWHM arising on the $\text{Im}[\chi_{SQD}^{(1)}]$ spectrum should both increase with the increase of the electron tunneling rate. This result is in accordance with the findings stemming from the comparison of Fig. 2 with Fig. 3, where the value of $\hbar T_e$ is taken equal to 0.15 meV . We also note that the slope of the linear dispersion spectrum $\text{Re}[\chi_{SQD}^{(1)}]$, at the position where the absorption is minimized, is steeper compared to the corresponding slope in the high tunneling rate regime, Fig. 2(a), that leads to the decrease of the group velocity of the propagated light within the SQD (see also Fig. 4). The substantial slowing-down of light combined with the quite narrow transparency window are consequences of the tunneling induced transparency [3], unlike in the case of the low electron tunneling regime, where the smooth slope and the broad transparency window originate from the Autler-Townes splitting effect [3].

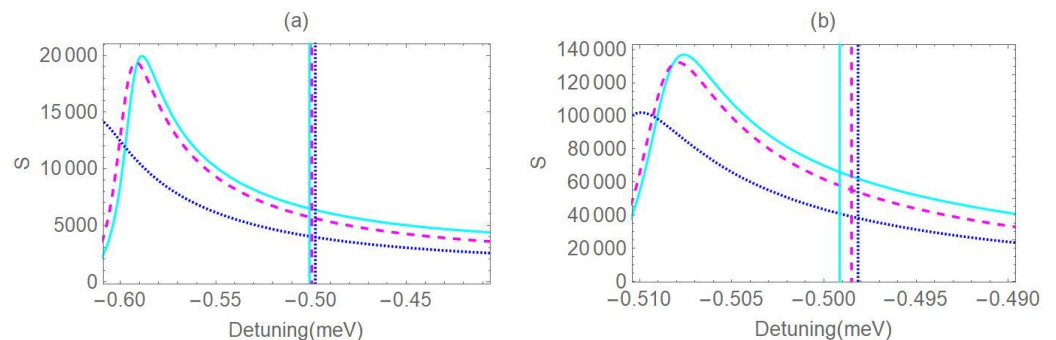


Figure 4. The slow-down factor, S , as a function of the field detuning, for the same values of the physical parameters as the ones used in Figs. 2 and 3, in captions (a) and (b), respectively. The vertical lines intersect the horizontal axis at the position where $\text{Im}[\chi_{MNP}^{(1)}]$ is minimized.

4. Conclusions

In summary, we theoretically explored the linear optical response of an asymmetric tunneling-controlled double SQD – MNP, to an incident electromagnetic field. We use a density matrix approach and calculate the real and imaginary parts of the linear optical susceptibility of the SQD in the presence of the MNP. We found that, in the high electron tunnelling regime, a broad transparency window originating from the Autler-Townes effect

arises on the absorption spectrum, that is approximately centered around a field detuning equal to the energy gap between the upper states of the double SQD molecule. In the low electron tunneling regime, the width of this transparency window diminishes, while the slope of the absorption spectrum increases. We can take advantage of this effect known as tunneling induced transparency for the precipitation of light within the medium. We also found that the decrease of the distance between the counterparts of the hybrid nanostructure induces the broadening of the transparency window.

Author Contributions: Conceptualization, S.G.K. and E.P.; methodology, S.G.K. and E.P.; software, S.G.K.; validation, S.G.K. and E.P.; investigation S.G.K. and E.P.; writing—original draft preparation, S.G.K. and E.P.; writing—review and editing; S.G.K. and E.P.; visualization, S.G.K.; supervision, E.P.; All authors have read and agreed to the publishes version of the manuscript.

Funding: This research received no external funding.

Institutional Review Board Statement: Not applicable.

Informed Consent Statement: Not applicable.

Data Availability Statement: The data presented in this study are available on request from the corresponding author.

Conflicts of Interest: The authors declare no conflict of interest.

References

1. Villas-Boas, J. M.; Govorov, A. O.; Ulloa, S. E.; Coherent control of tunneling in a quantum dot molecule. *Phys. Rev. B* **2004** *69*, 125342.
2. Borges, H. S.; Sanz, L.; Villas-Boas, J. M.; Alcalde, A. M.; Robust states in semiconductor quantum dot molecules. *Phys. Rev. B* **2010** *81*, 075322.
3. Yao, H.-F.; Cui, N.; Niu, Y.-P.; Gong, S.-Q.; Voltage-controlled coherent population transfer in an asymmetric semiconductor quantum dot molecule. *Photonics Nanostruct. Fundam. Appl.* **2011** *9*, 174-178.
4. Voutsinas, E.; Terzis, A. F.; Paspalakis, E.; Control of indirect exciton population in an asymmetric quantum dot molecule. *Phys. Lett. A* **2014** *378*, 219-225.
5. Yuan, C.-H.; Zhu, K.-D.; Voltage-controlled slow light in asymmetry double quantum dots. *Appl. Phys. Lett.* **2006** *89*, 052115.
6. Borges, H. S.; Sanz, L.; Villas-Bôas, J. M.; Diniz Neto, O. O.; Alcalde, A. M.; Tunneling induced transparency and slow light in quantum dot molecules. *Phys. Rev. B* **2012** *85*, 115425.
7. You, Y.; Qi, Y. H.; Niu, Y.-P.; Gong, S.-Q.; Control of electromagnetically induced grating by surface plasmon and tunneling in a hybrid quantum dot-metal nanoparticle system. *J. Phys.: Condens. Matt.* **2019** *31*, 105801.
8. Kosionis, S.G.; Paspalakis, E.; Controlling the pump-probe optical response in asymmetric tunneling-controlled double quantum dot molecule—metal nanoparticle hybrids. *Applied Sciences* **2021** *11*, 11714.
9. Akram, H.; Abdullah, M.; Al-Khursan, A. H.; Energy absorbed from double quantum dot-metal nanoparticle hybrid system, *Scient. Rep.* **2022** *12*, 21495.
10. Kosionis, S.G.; Paspalakis, E.; Coherent effects in energy absorption in double quantum dot molecule—Metal nanoparticle hybrids. *Physica E: Low-dimensional Systems and Nanostructures* **2022** *135*, 114907.
11. Johnson, P. B.; Christy, R. W.; Optical constants of the noble metals. *Phys. Rev. B* **1972** *6*, 4370.